Supporting Information

Controllable Synthesis of Variable-sized Magnetic Nanocrystals Self-assembled into Porous Nanostructures for Enhanced Cancer Chemo-ferroptosis Therapy and MR Imaging

*Jianxiang Xu [a #], Hanyuan Zhang [b#], Yifei Zhang [c], Xu Zhang [a], Teng Wang [a], Shi Hong [a], Wenmei Wei [a], Tingting Zhao [a *], Weijun Fang [a *]*

[a] School of Basic Medical Sciences, Anhui Medical University, Hefei 230032, Anhui, China

[b] Department of Orthopedics, Department of Sports Medicine and Arthroscopic Surgery, The First Affiliated Hospital of Anhui Medical University, Hefei 230022, China

[c] Department of Orthopaedics, The Third Affiliated Hospital of Anhui Medical University, Hefei 230061, China

[#] These authors contributed equally to this work.

Corresponding Author

*(Weijun Fang) E-mail: fangweijun@ahmu.edu.cn; wjfang81@163.com

Phone: +86551 65161138

* (Tingting Zhao) E -mail: ttzhao@ahmu.edu.cn

Experimental section

Materials and chemicals: $FeCl_3 \cdot 6H_2O$, $MnCl_2 \cdot 4H_2O$, sodium acetate (NaOAc), H_2O_2(30%), ethylene glycol (EG) and polyethylene glycol 600(PEG600) were obtained from Sinopharm Chemical Reagent Co. Ltd. (Shanghai, China). Doxorubicin (DOX) and 3,3,5,5-tetramethylbenzidine (TMB) were ordered from Aladdin (China). 2,7-dichlorofluorescein diacetate (DCFH-DA) fluorescence probe and 3-(4,5)-dimethyl-2-thiahiazoyl)-2,5-diphenyltetrazolium bromide (MTT) were purchased from Sigma. The human HepG2 cells were maintained in Duibecco's modifified Eagle's medium (DMEM) supplemented with 10% fetal bovine serum, at 37 ℃, 5% CO_2. DMEM and fetal bovine serum were ordered from Hyclone (USA). The other chemicals were of analytical grade and used without further purification. All animal experiments operations were performed in accordance with the guidelines of the Institutional Animal Care and Use Committee (IACUC) and the care regulations approved by the Administrative Committee of Laboratory Animals of Anhui Medical University (NO. LLSC20210778).

Synthesis of porous Mn-doped Fe_3O_4 NPs with tunable grain sizes: 270 mg of $FeCl_3 \cdot 6H_2O$, 99 mg of $MnCl_2 \cdot 4H_2O$ and 959 mg of NaOAc were dissolved in a mixture of EG and PEG600 (V_{EG}:V_{PEG600} = 1:1, total volume = 20 mL) under magnetic stirring. After that, a desired amount of water [i.e., a: 0 μL (0 mmol, Mn(0.25)-Fe_3O_4-I NPs), b: 170 μL (9.4 mmol, Mn(0.25)-Fe_3O_4-II NPs), c: 304 μL (16.9 mmol, Mn(0.25)-Fe_3O_4-III NPs), c: 800 μL (44.4 mmol, Mn(0.25)-Fe_3O_4-IV NPs)]was added into the mixture. The mixture solution was then transferred into a Teflon-lined stainless-steel autoclave and heated to 200℃. After reaction for 6 h, the autoclave was cooled to room temperature. The Mn(0.25)-Fe_3O_4 NPs were collected by a magnet and washed with ethanol and ultra-pure water. To control the level of Mn^{2+} doping ((Mn_xFe_{1-x})Fe_2O_4 , x= 0, 0.14, 0.21, 0.25 and 0.30), different amount of Mn^{2+} chloride precursors (0 mg,

39.6 mg, 79.2 mg, 99 mg and 148.5 mg) were used under the same conditions as mentioned above.

DOX loading capacity and release behavior: The loading of DOX into the porous Mn(0.25)-Fe_3O_4-III NPs was determined using a UV-vis spectrometer via measuring absorption at 479 nm. Briefly, 10 mg of porous Mn(0.25)-Fe_3O_4-III NPs was mixed with 0.5 mg of DOX in ultra-pure water. The mixture solution was kept overnight under vigorous shaking to get DOX/Mn(0.25)-Fe_3O_4-III NPs. Unbound DOX was wiped off and quantified by analyzing the absorbance of the supernatant at a wavelength of 479 nm.

To study the DOX release behavior, 2 mg of DOX/Mn(0.25)-Fe_3O_4-III NPs was dispersed in 1 mL PBS buffer at different pH values (pH = 7.4 and 6.0) with gently shaking at 37℃. At each time point, the release medium was collected for UV-vis spectrometer measurements and fresh medium was supplied.

In vitro peroxidase-like activities tests: Porous Mn(0.25)-Fe_3O_4-III NPs (20 μg/mL) and TMB (0.1 mg/mL) were added into HAc buffer (0.1 M, pH = 4.8). The peroxidase-like activity was monitored immediately after adding different concentrations of H_2O_2 (40, 60, 80 and 100 mM) into the above solutions. The data were collected by recording the absorption of the solutions at 650 nm on time-scan mode through a UV-vis-NIR spectrophotometer. Under the same condition, the reaction solution without porous Mn(0.25)-Fe_3O_4-III NPs was also tested.

In vitro catalase-like activities tests: Porous Mn(0.25)-Fe_3O_4-III nanoparticles (20 μg/mL) were dispersed in 4.0 mL of HAc buffer (0.01 M, pH = 7.4) containing different concentration of H_2O_2 (40, 60, 80 and 100 mM) at room temperature. The dissolved oxygen concentrations were tested by a dissolved oxygen meter (SX716, Shanghai San-Xin Instrumentation, China).

Cellular uptake of the porous Mn(0.25)-Fe_3O_4-III NPs: HepG2 cells were seeded in a 24-well plate (~0.5×10^5 cells per well) and incubated with porous Mn(0.25)-Fe_3O_4-III NPs (0, 25

and 50 ppm) for 6 h. Followed, the cells were washed with PBS, stained with prussian blue (50 ppm, 20 min) and then photographed.

To investigate the Mn(0.25)-Fe_3O_4-III NPs cellular endocytosis, HepG2 cells were washed , fixed with 2.5 % glutaraldehyde, post-fixed in 1% osmium tetroxide, dehydrated in ethanol, and infiltrated with resin. Then, the samples were sliced with a diamond knife. The ultrathin sections (~70 nm) were supported on a copper grid and examined with a TEM (Talos L120C G2, USA).

Detection of intracellular ROS Generation: HepG2 cells were seeded in a 6-well plate and cultured for 24 h. The cell medium was removed, and replaced by fresh cell medium containing porous Mn(0.25)-Fe_3O_4-III NPs (0, 50, 75 and 100 ppm) for another 12 h. H_2O_2 (60 mM) was added into cell media and incubated for 6 h, following by washing with PBS and incubated with 5 mM DCFH-DA for 30 min. Fluorescence intensity was analyzed by a flow cytometer (BD FACSVerse, Ex = 488 nm, Em = 525 nm).

For fluorescence imaging, HepG2 cells were seeded in a 24-well plate (~0.5×10^5 cells/well) and incubated with porous Mn(0.25)-Fe_3O_4-III NPs (0 and 10 ppm) for 12 h. H_2O_2 (60 mM) was added into cell media and incubated for 6 h, following by washing with PBS and incubated with 10 mM DCFH-DA for 30 min. Cell imaging was then carried out by fluorescence microscope after washing cells with PBS.

In vitro antitumor efficacy of DOX/Mn(0.25)-Fe_3O_4-III NPs: HepG2 cells were seeded in a 96-well plate at the amount of 10^4 cells/well overnight for adherence. Then, the cells were exposed to free DOX and DOX/Mn(0.25)-Fe_3O_4-III NPs at desired concentration. After 12 h incubation, cell viabilities were tested by standard MTT assay.

To study that the DOX/Mn(0.25)-Fe_3O_4-III NPs could efficiently kill cancer cell by ROS-induced ferroptosis, the cells were incubated with Mn(0.25)-Fe_3O_4-III NPs and DOX/Mn(0.25)-Fe_3O_4-III NPs for 12 h. The cell medium was removed and rinsed with medium, and 60 μM H_2O_2 was then added. Cells were incubated in fresh medium (pH = 6.0) for another 6 h prior to

being further analyzed by MTT assay. To identify the cell viability, the dead cells were stained with Trypan Blue.

Magnetic resonance imaging (MRI): Porous Mn(0.25)-Fe_3O_4-III NPs at given total metal ions (Fe and Mn) concentrations of 0.6 mM, 0.3 mM, 0.15 mM, 0.075 mM and 0.0375 mM were dispersed in ultra-pure water containing 1% agar gel for MRI scanning. Both the T_2-weighted MR images and relaxation time T_2 values were obtained using a 9.4 T MRI magnet (Bruke 9.4T MicroMRI).

For *in vivo* magnetic resonance imaging, mice bearing tumors were injected with porous Mn(0.25)-Fe_3O_4-III NPs solution (50 μL, 2.2 mg/kg) or PBS (50 μL). After 2 h, the mice were scanned by 9.4 T MRI scanner at T_2-weighted MR imaging mode with the following parameter: TR/TE = 2000/10 ms, 256×256 matrices, repetition times = 4.

In vivo antitumor efficacy of DOX/Mn(0.25)-Fe_3O_4-III NPs: HepG2 cells (5×10^6) in 100 μL PBS solution were subcutaneously injected into the right flank of each female Babl/c mouse (4 weeks, ~16 g). After the tumor formation to approximately 50-60 mm^3, the mice were randomly divided into five groups (five mice for each group). Group I: PBS (injection of 100 μL); group II: H_2O_2 (injection of 100 μL, 1.5 mg kg^{-1}, the injections of H_2O_2 were performed every three days); group III: free DOX (injection of 100 μL, 10 mg kg^{-1} DOX); group IV: Mn(0.25)-Fe_3O_4-III NPs + H_2O_2 (injection of 100 μL, the injections of H_2O_2 were performed every three days); group V: DOX/Mn(0.25)-Fe_3O_4-III NPs (injection of 100 μL,10 mg kg^{-1} DOX); group VI: DOX/Mn(0.25)-Fe_3O_4-III NPs + H_2O_2 (DOX/Mn(0.25)-Fe_3O_4-III NPs: injection of 100 μL, 10 mg kg^{-1} DOX; H_2O_2: injection of 100 μL, 1.5 mg kg^{-1}, the injections of H_2O_2 were performed every three days). During the treatment, tumor volumes and body weights were monitored every two days to estimate the therapeutic performance. The tumor inhibition ratio (IR) was also calculated according to the following expression:

$$IR(\%) = \frac{Vc - Vt}{Vc} \times 100\% \qquad (1)$$

Where V_c is the average tumor volume of control group after treated with PBS for 15 days (group I) , and V_t is the average tumor volumes of treatments (group II, group III, group IV, group V and group VI). After 15 days of treatment, the mice were euthanized and their major organs (heart, liver, spleen, lung and kidneys) were removed, and stained with hematoxylin and eosin (H&E) for histological analysis.

Statistical analysis: Results were presented as the mean ± standard deviation (SD). Statistical significance was performed via one-way Student's t test. $P < 0.05$ was considered statistically significant.

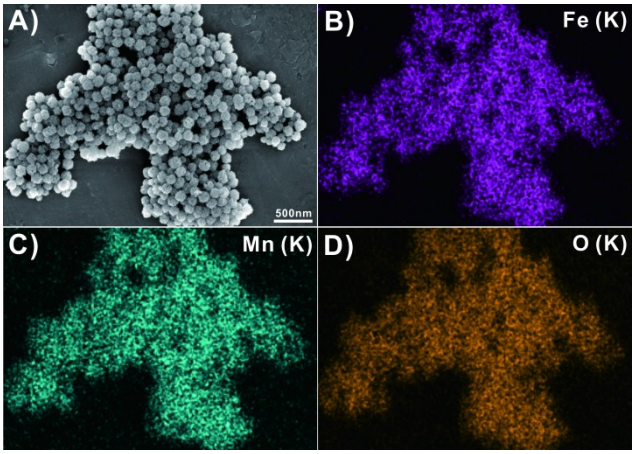

Figure S1. SEM image (A) and Fe/Mn/O (B, C, and D) elemental mapping of the obtained Mn(0.25)-Fe_3O_4-III nanoparticles. The chemical compositions of the Mn(0.25)-Fe_3O_4-III nanoparticles were identified as $(Mn_{0.25}Fe_{0.75})Fe_2O_4$ by inductively coupled plasma-atomic emission spectrophotometer (ICP-AES).

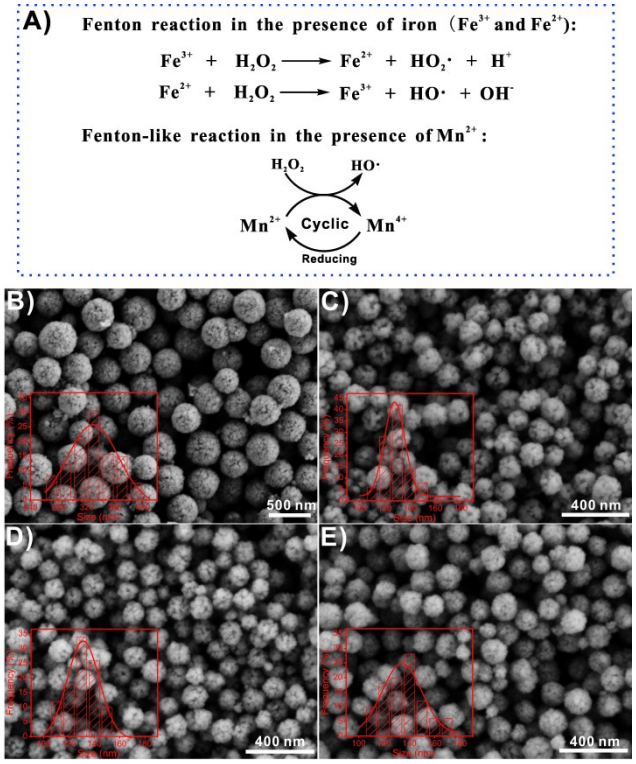

Figure S2. A) Mechanisms of Fenton and Fenton-like reactions in the presence of iron (Fe^{3+} and Fe^{2+}) and manganese (Mn^{2+}) ions. SEM images of the porous magnetic nanoparticles with different Mn doping: B) Fe_3O_4 NPs , C) $(Mn_{0.14}Fe_{0.86})Fe_2O_4$ NPs, D) $(Mn_{0.21}Fe_{0.79})Fe_2O_4$ NPs and E) $(Mn_{0.30}Fe_{0.70})Fe_2O_4$ NPs. Inset: the corresponding particle sizes distribution.

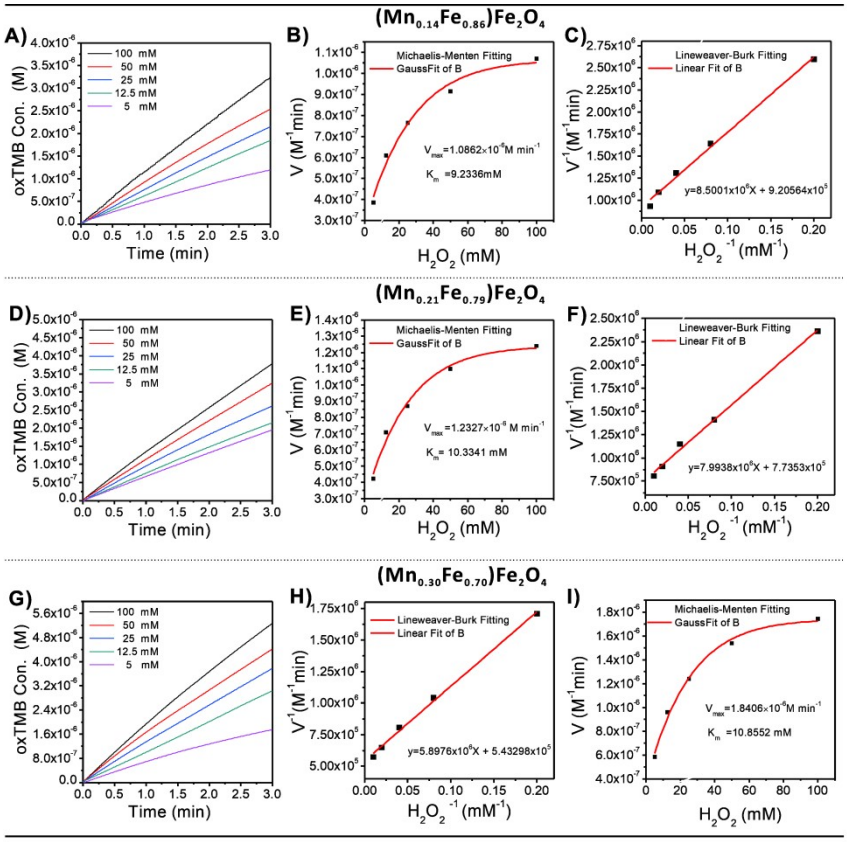

Figure S3. Linear fitting of the concentration of oxTMB against time in the first 3 minutes for $(Mn_{0.14}Fe_{0.86})Fe_2O_4$ NPs (A), $(Mn_{0.21}Fe_{0.79})Fe_2O_4$ NPs (D) and $(Mn_{0.30}Fe_{0.70})Fe_2O_4$ NPs (G). The slope is used to calculate initial velocities. Michaelis-Menten kinetics (B, E and H) and Lineweaver-Burk plotting (C, F and I) for the corresponding nanoparticles with H_2O_2 as substrate.

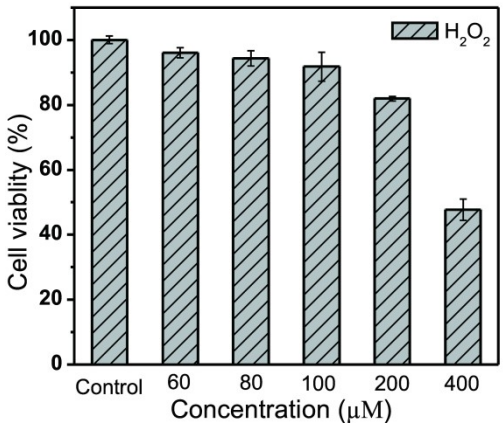

Figure S4. Relative viability of HepG2 cells incubated with H_2O_2 at different concentrations.

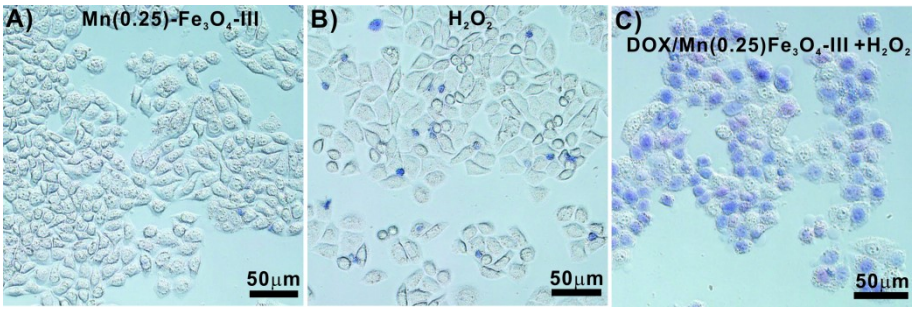

Figure S5. Micrographs of trypan blue-stained HepG2 cells in the present of A) Mn(0.25)-Fe_3O_4-III, B) H_2O_2 and C) Mn(0.25)-Fe_3O_4-III + H_2O_2. The dead cells were stained into purple by the trypan blue.

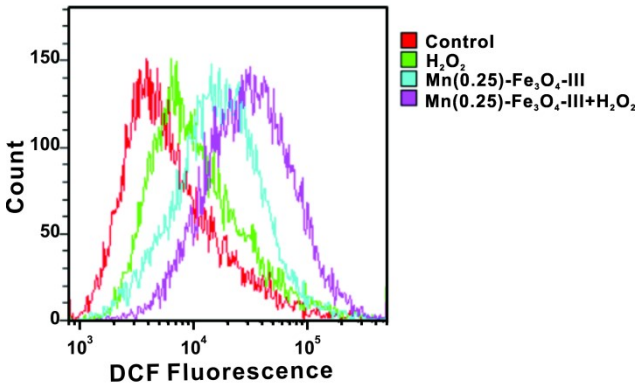

Figure S6. Flow cytometric analysis of intracellular ·OH levels in HepG2 cells incubated with H_2O_2 , Mn(0.25)-Fe_3O_4-III and Mn(0.25)-Fe_3O_4-III + H_2O_2. HepG2 cells were stained by the fluorescence probe 2',7'-dichlorofluorescin diacetate (DCFH-DA), which could be oxidized by intracellular ·OH to emit green fluorescence.